# A High Efficiency DC-DC Converter Topology Suitable for Distributed Large Commercial and Utility Scale PV Systems

Mohammed S. Agamy, Maja Harfman-Todorovic, Ahmed Elasser, Robert L. Steigerwald, Juan A. Sabate, Song Chi, Adam J. McCann, Li Zhang, and Frank Mueller

GE Global Research Center Niskayuna, NY, USA

Abstract — In this paper a DC-DC power converter for distributed photovoltaic plant architectures is presented. The proposed converter has the advantages of simplicity, high efficiency, and low cost. High efficiency is achieved by having a portion of the input PV power directly fed forward to the output without being processed by the converter. The operation of this converter also allows for a simplified maximum power point tracker design using fewer measurements

*Keywords* — Distributed PV Architectures; Partial Power Processing; Buck-Boost Converter; Maximum Power Point Tracking

### I. INTRODUCTION

Distributed photovoltaic power plants provide several advantages over the standard central inverter systems, including: higher energy yield, more flexibility in plant design, and improved monitoring and diagnostics capabilities [1-16]. Studies show that the distribution of DC-DC converters along with the maximum power point tracking (MPPT) controllers associated with them at the string level, as shown in Fig. 1, provides a significant increase in the annual energy yield of the system of 6% to 8% in utility and large scale commercial systems [3], which is more than enough to compensate for the cost of the additional power electronics.

A trade-off study including detailed energy yield, reliability, and cost analysis showed that a selection of a string level MPPT architecture (Fig. 1.c) is the best approach for large commercial installations and utility scale PV systems (200 kW up to 2 MW).

One of the key factors affecting the distributed PV system design is the proper selection and design of the DC-DC converters used in these architectures. Using converters of smaller power ratings leads to a decrease in conversion efficiency as well as an increase in cost per unit power as compared to large centralized converters. This has to be taken into account to ensure that the benefits of distributing the DC-DC converters in a PV plant are not offset by the drop in conversion efficiency. DC-DC converter efficiencies in the order of 98% and higher are needed such that the gains in energy yield obtained by distributing the DC-DC power conversion stage does not get cancelled out by the drop in power converter efficiency. In this paper, a high efficiency

partial power buck-boost DC-DC converter is presented for use in distributed PV systems based on its performance, reliability, and estimated cost.

Based on the comparative system study in [3], power converters at the string or multi-string level show (1.5 kW~6 kW rated power) best the performance/cost trade-off point. Therefore, a 3.5 kW DC-DC converter design is proposed in this paper. The input to the converter can be either one mc-Si string or multiple CdTe or CIGS strings. The converter is composed of two interleaved 1.75 kW channels to reduce input current ripple. Efficiency is maximized by using a partial power processing scheme as well as operating only one of the two interleaved channels at light loads. Furthermore, in very light load conditions the converter is operated in discontinuous conduction mode to reduce device turn on losses.

# II. CONVERTER OPERATION & DESIGN

One way to improve efficiency of the DC-DC converters is by means of using partial power processing, as shown in Fig. 2 [17-23]. In these converters, part of the input power is directly fed forward to the output, thus achieving close to 100% efficiency, the remaining part of the power processed by the DC-DC converter is determined by the voltage regulation requirements, i.e. the percentage of power processed by the converter depends on the voltage difference between the PV side and the DC-link voltage, Fig. 3 shows the relation between the required voltage gain and the percentage of input power being processed by the converter. With a proper design, the power converter can be designed to handle around 30~ 40% of the input power at nominal operating conditions, thus improving its cost, size and efficiency. Therefore, the DC-DC converter block does not need to have excessively high efficiency over its operating range to achieve overall high conversion efficiency. An example of this is shown in Fig. 4, where a DC-DC converter with an assumed efficiency of 95% leads to an overall efficiency above 98% for input voltages that are equal to 60% or higher of the output DC-link voltage when used in a partial power conversion mode.

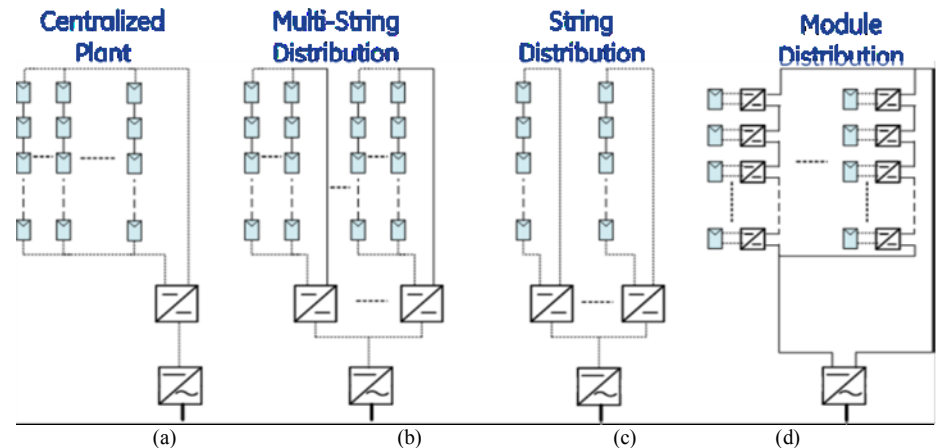


Fig. 1 PV plant architectures: (a) Centralized, (b) Multi-string distribution, (c) String distribution and (d) Module distribution

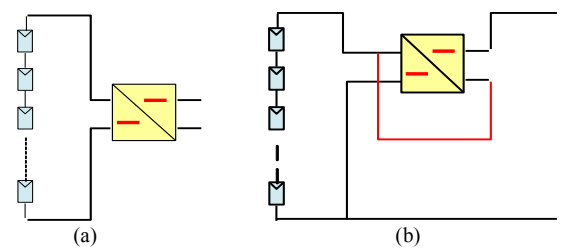


Fig. 2 (a) Full power vs. (b) Partial power processing structures

For string converters rated at (1.5 kW~6 kW), the estimated gain in energy yield is in the range of 3%~9% over a standard central inverter system, therefore, a target composite efficiency of 98% is needed in order not to have a significant negative impact on the annual yield. This composite efficiency is based on the California Energy Commission (CEC) weighted efficiency formula for solar inverters.

$$\begin{split} \eta_{CEC-weighted} &= 0.04 \eta_{10\%} + 0.04 \eta_{20\%} + 0.12 \eta_{30\%} + 0.21 \eta_{50\%} + \dots \\ &\qquad \qquad \dots + 0.53 \eta_{75\%} + 0.05 \eta_{100\%} \end{split}$$

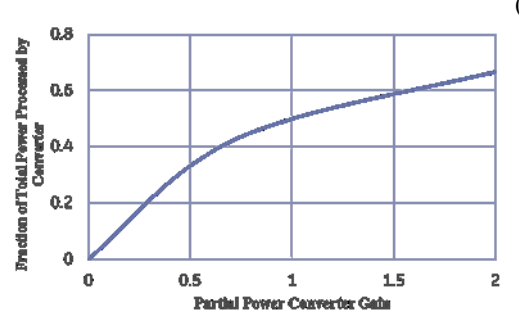


Fig. 3 Fraction of total power processed vs. voltage gain for a partial power converter

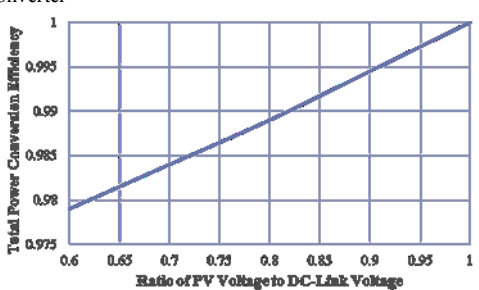


Fig. 4 An example of overall efficiency of a partial power conversion topology assuming a 95% DC-DC converter efficiency

The DC-DC converter presented in this paper is a partial power processing buck-boost converter as shown in Fig. 5 (a). In this topology, the output voltage is the sum of the PV string voltage and the voltage of the output capacitor. Since this converter does not need to process all the input power, the overall conversion efficiency is quite high. The converter has a very simple topology composed of only one switching device and one diode per channel. The switches and diodes have to withstand the total output voltage. The voltage gain of the regulated voltage Vs at medium to heavy loading conditions (in CCM operation) is given in equation (2), which is the conversion ratio of a non-inverting buck-boost converter.

$$V_{s} = \frac{d}{1 - d} V_{in} \tag{2}$$

In discontinuous conduction mode, the capacitor voltage is given by,

$$V_{s} = \frac{1}{2} \left( \sqrt{1 + \frac{2dR_{load}}{L_{in}f_{sw}}} - 1 \right) V_{in}$$
 (3)

And the fraction of input power processed by the converter is given by:

Fraction of Power Processed = 
$$\frac{\left(\frac{V_s}{V_{in}}\right)}{\left(\frac{V_s}{V_{in}}+1\right)}$$
 (4)

The operation of the converter is similar to that of a simple boost circuit. The stages of operation over a switching period (T<sub>s</sub>) are shown in Fig. 6 and can be summarized as follows:

Stage 1 (0 < t <  $dT_s$ ): in this stage IGBT (S) is turned on and the inductor current builds up.

$$L_{in}\frac{di_{Lin}}{dt} = V_{in} \tag{5}$$

$$L_{in} \frac{di_{Lin}}{dt} = V_{in}$$

$$C_{s} \frac{dV_{s}}{dt} = -\frac{V_{s} + V_{in}}{R_{load}}$$
(6)

Stage 2 ( $dT_s < t < T_2$ ): the IGBT is turned off and the inductor current is diverted to the diode (D) where the energy is discharged into the capacitor Cs. For continuous conduction mode T<sub>2</sub>=T<sub>s</sub>, and the cycle ends at this stage.

$$L_{in}\frac{di_{Lin}}{dt} = -V_s \tag{7}$$

$$C_{s} \frac{dV_{s}}{dt} = i_{Lin} - \frac{V_{s} + V_{in}}{R_{load}}$$
(8)

Stage 3 ( $T_2 < t < T_s$ ): this stage occurs in the case of discontinuous inductor current conduction mode (DCM). In this mode power is transferred from the input and output capacitors to the output.

$$L_{in}\frac{di_{Lin}}{dt} = 0 (9)$$

$$L_{in} \frac{di_{Lin}}{dt} = 0$$

$$C_{s} \frac{dV_{s}}{dt} = -\frac{V_{s} + V_{in}}{R_{load}}$$
(10)

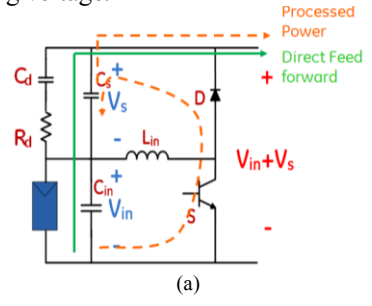
It is also worth noting that during this mode of operation resonances can occur between the input inductor and device capacitance. The DCM operation leads to zero current turn on of the IGBT thus reducing the turn on losses at light load.

In light load conditions, the converter can be designed to transition to critical conduction mode and then DCM to reduce power losses at turn on. The input inductor value can be chosen as a function of converter power and operational duty ratio as shown in Fig. 7. Fig. 8 shows the loss breakdown of the DC-DC converter at rated design conditions (3.5 kW, 400 V input), indicating the dominance of the IGBT switching losses over all the other loss components. Diode losses are primarily conduction losses since SiC Schottky diodes are used to eliminate reverse recovery losses.

A 3.5 kW two-channel interleaved converter is shown in Fig. 5 (b). When the input PV power is less than 50% of the rating, the switching is stopped in one of the channels. Thus eliminating all the associated switching losses and improving light load efficiency. Operation can be alternated between the two channels in order to improve the reliability of the converter.

Converter control is based on having an output constant DC voltage. The DC-link voltage is controlled by the DC-AC inverter modulation. The duty cycle (d) is calculated to adjust the PV string voltage Vin such that the maximum power of the PV string/array can be tracked. In this case Vs is determined in order to compensate the difference between the PV voltage Vin and the output DC-link voltage. The input voltage command Vin Cmd is calculated by the MPPT controller. With a constant output DC-link voltage Vout, the MPPT control can be simplified to maximize the output current Iout through perturbing the input PV voltage Vin. There is no power calculation required in this algorithm, thus reducing computation complexity and time. Fig. 9 shows a simplified block diagram of the converter controller.

In addition to the MPPT control, it can also be used for monitoring and diagnostics of the PV strings and the DCnetwork in the plant, fault detection, as well as clamping the PV string voltage.



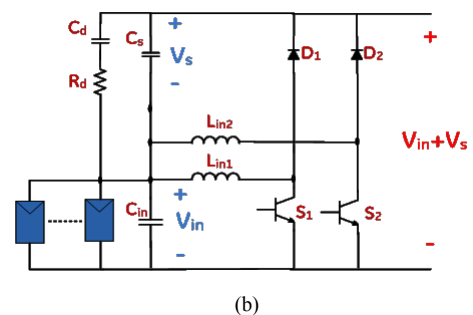


Fig. 5: A buck-boost partial power DC-DC converter with a Si IGBT and a SiC Schottky diode. One channel is rated at 1.75 kW. Input Voltage: 200 V to 600 V, Output Voltage: 600 V regulated. a) one channel; b) two channels

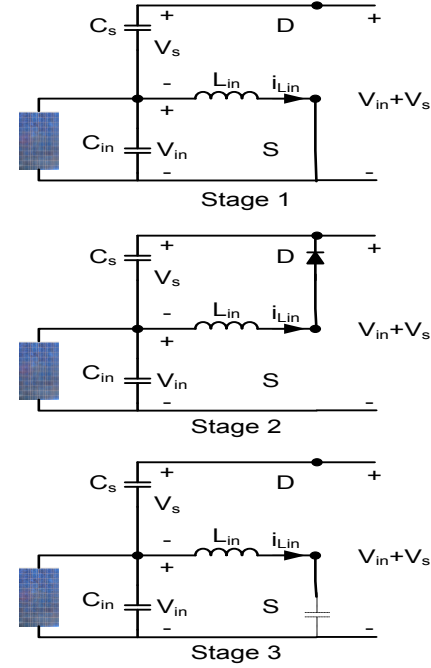


Fig. 6 Stages of operation of the partial power processing DC-DC converter

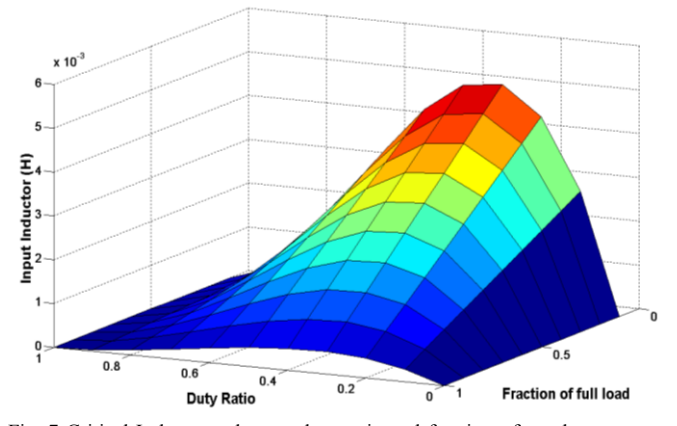


Fig. 7 Critical Inductor value vs. duty ratio and fraction of rated power at 30 kHz switching frequency

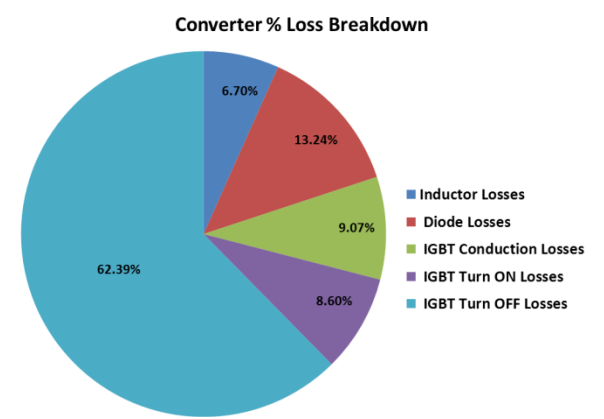


Fig. 8 Converter loss breakdown as a percentage of the total losses at nominal operating conditions

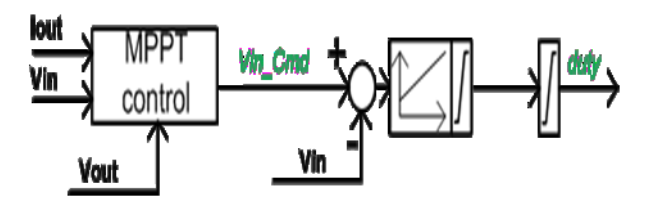


Fig.9 Simplified block diagram of the controller including the MPPT control block

#### III. EXPERIMENTAL RESULTS

A 3.5 kW, 30 kHz, two channel DC-DC converter prototype as shown in Fig. 10, was built and tested. Converter component values are listed in Table I. The converter power density is 19.5W/in<sup>3</sup>. SiC Schottky diodes are used for D<sub>1</sub> and D<sub>2</sub> in order to avoid reverse recovery losses at high frequency. The input PV voltage ranges from 200 V - 600 V, while the output voltage is fixed at 600 V, which is regulated by the grid tied DC-AC inverter stage. Converter efficiency evaluation was performed using a variable input DC voltage (200 V-480 V) and an electronic load operating in fixed voltage mode with a set point of 600 V. Efficiency measurements were performed across the full load range (10%-100%) in order to generate the composite weighted efficiency number for solar converters as given in eq. (1). As seen in Fig. 11, the composite efficiency of each individual channel exceeds 98% with a peak efficiency reaching 98.9%. The number of channels operated is decided by the input power, therefore, for power levels less than 50% of the converter rating only one channel is switched. This improves the efficiency profile, giving a composite weighted efficiency of 98.22%, as shown in Fig. 12. The converter was then tested with a PV emulator input and its output connected to the DC-link of a grid tied inverter as shown in Fig. 13. Interleaved inductor currents and the resulting low ripple input current are shown in Fig. 14(a). CCM operation at high input power and DCM operation at low input power are shown in Fig. 14(b) and Fig. 14(c) respectively.

Global MPPT sweep is performed, as shown in Fig. 15 to locate the absolute maximum output power by sweeping the PV voltage from its open circuit value, to a set minimum value (200 V in this test). Since the output voltage is constant, the output current profile during the sweep matches the PV (power-voltage profile). Finally, the MPPT performance was studied by using the PV

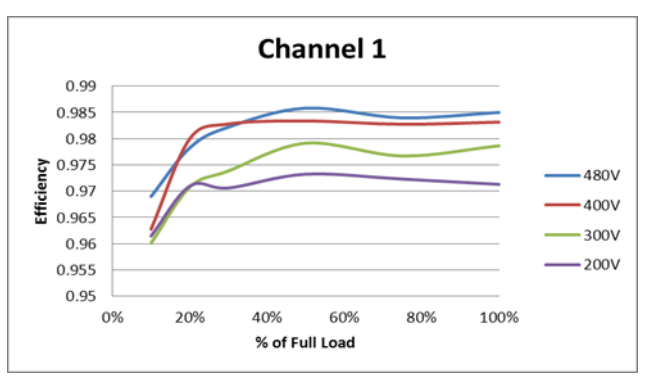
emulator to apply a transient irradiance profile, as shown in Fig. 16(a) to the PV string characteristic. Fig. 16(b) shows the power extracted from the PV string and the tracking efficiency of the MPPT controller. At low power levels only one channel is switched and as the input PV power increases both channels are operated. The MPPT efficiency achieved is above 99.7% in static condition and during fast transients it remains above 96%, which guarantees high PV energy extraction.

TABLE I CONVERTER COMPONENTS

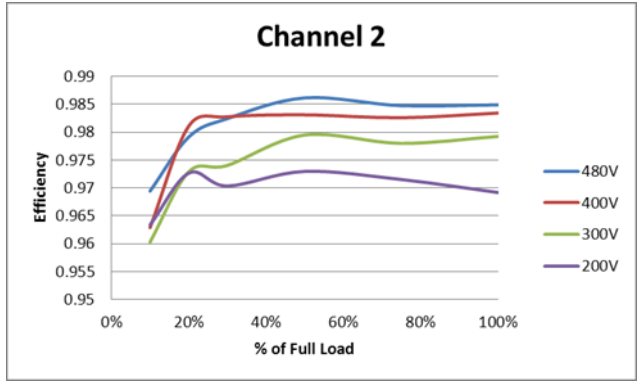
Switching Frequency	30 kHz
Rated Power	3.5 kW (1.75 kW/channel)
$L_{in}$	600 uH
$C_s$	30 uF
$C_{in}$	60 uF
$S_1, S_2$	1KW40N120H3
$D_1, D_2$	C2D20120D



Fig. 10 Prototype of the 3.5 kW (two channels)



Composite Efficiency 98.0421%



Composite Efficiency 98.0908%

Fig. 11 Measured efficiency for different input power, input voltages, and converter configurations

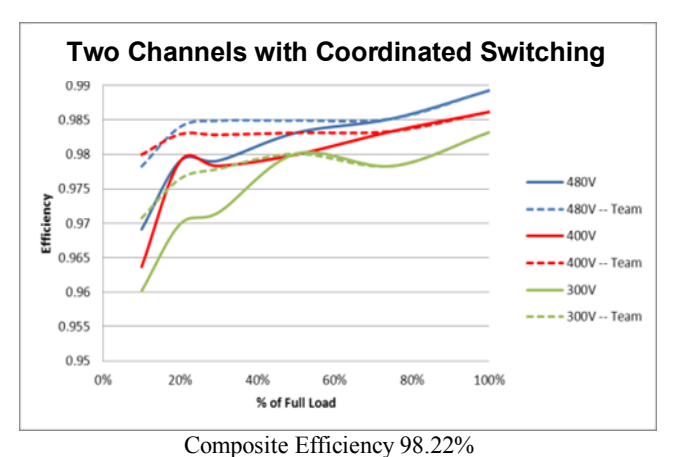


Fig. 12 Efficiency improvement due to coordinated switching of the two channels (Solid lines two channels switching, Dotted lines: one channel switched off at light load)

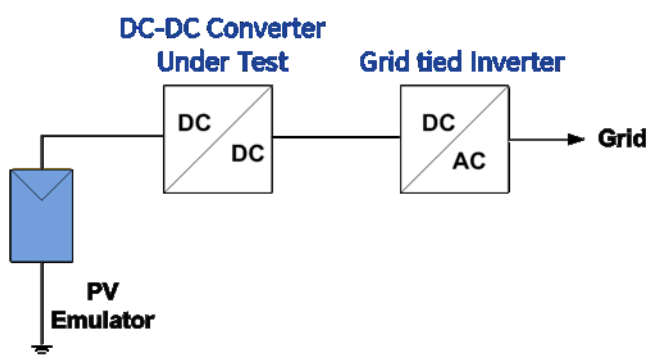
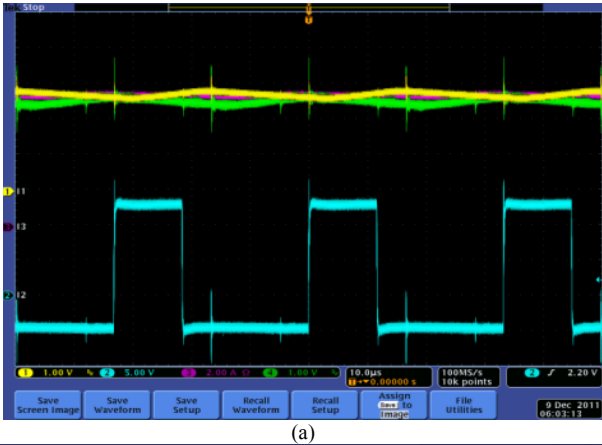
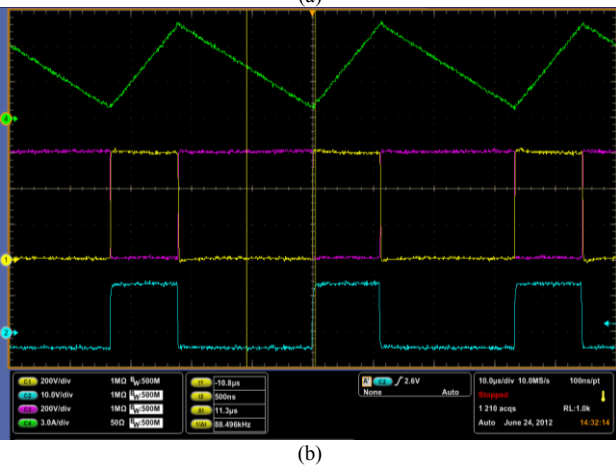


Fig. 13 Block diagram of converter test setup





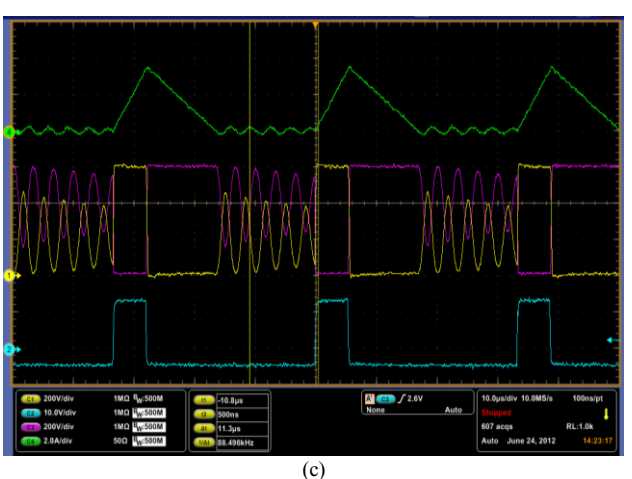


Fig. 14 Converter waveforms in different conditions: (a) interleaved inductor currents (yellow & green, LEM output 1 V/div~1.6 A/div) total input current (magenta, 2 A/div) and gate of  $S_1$  (blue, 5 V/div), at input of 2 kW (b) IGBT voltage (yellow, 200 V/div), diode voltage (magenta, 200 V/div) and inductor current (green, 3A/div) of one channel, at total input of 1.75 kW and gate of  $S_1$  (blue, 10 V/div) and (c) IGBT voltage (yellow, 200 V/div), diode voltage (magenta, 200V/div) and inductor current (green, 2A/div) and gate of  $S_1$  (blue, 10 V/div) of one channel, at total input of 700 W

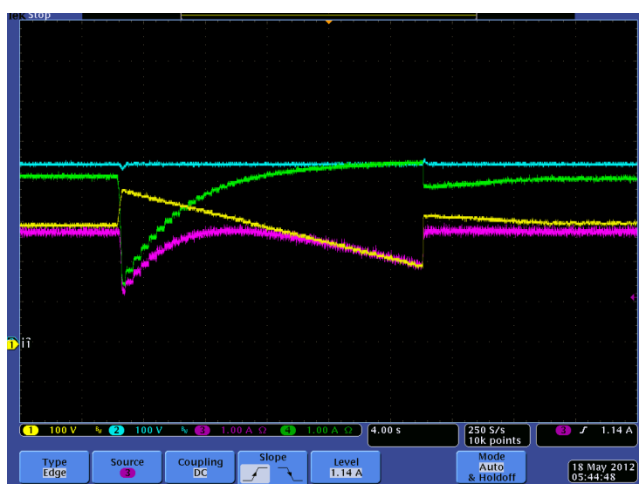
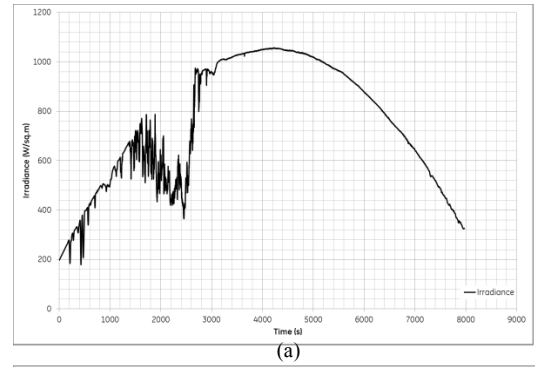


Fig. 15 Converter waveforms during a global MPPT sweep: Ch1 (yellow): PV input voltage (100 V/div), Ch2 (blue): Output voltage (100 V/div), Ch3 (magenta): Converter output current (1 A/div), Ch4 (green): Input PV current (1 A/div)

## IV. CONCLUSION

A simple high efficiency DC-DC converter suitable for medium to large scale distributed PV applications is proposed. High efficiency is achieved by means of partial power processing as well as by coordinating the operation of the interleaved channels of the converter. The output of the converter being a fixed DC-bus also simplifies the MPPT implementation. Furthermore, feedback signals can be used as monitoring and diagnostics tools for assessing the condition of the PV plant. Converter was fully tested for performance parameters including the efficiency, mode switching operation and MPPT performance for the static and dynamic conditions. Experimental results show excellent performance and fulfillment of the design parameters. Converter was also tested in a solar field and showed uninterrupted performance over a long period of time under varying environmental conditions. These results will be presented in the follow-up publication.



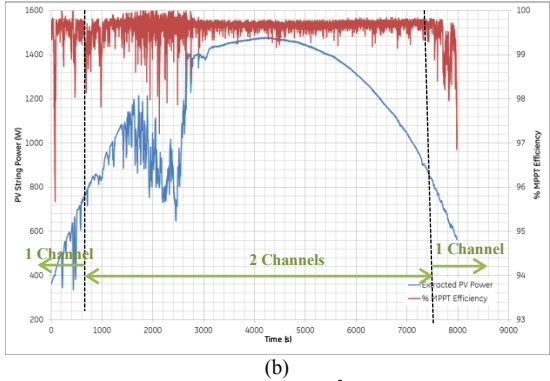


Fig. 16 (a) Irradiance profile (200 W/m<sup>2</sup>/div and (b) Extracted PV power (blue, 200 W/div) and MPPT efficiency (red, %)

#### ACKNOWLEDGMENT

This material is based upon work supported by the Department of Energy-Golden Field Office under Award DE-EE0000572.

# REFERENCES

- N. Kaushika & N. Gautam, "Energy Yield Simulations of Interconnected PV Arrays," IEEE Transactions on Energy Conversion, Vol.18, No. 1, May 2003, pp. 127-134.
- N. Femia, G. Lisi, G. Petrone, G. Spagnuolo & M. Vitteli, "Distributed Maximum Power Point Tracking of Photovoltaic Arrays: Novel Approach and System Analysis," Transactions on Industrial Electronics, Vol. 55, No. 7, July 2008, pp. 2610-2621
- A. Elasser, M. Agamy, J. Sabate, R. Steigerwald, R. Fisher & M. Harfman-Todorovic, "A Comparative Study of Central and Distributed MPPT Architectures for Megawatt Utility and Large Scale Commercial Photovoltaic Plants," Proceedings of Industrial Electronics Conference (IECON) 2010. pp. 2753-2758.
- G. Lijun, R. Dougal, L. Shengyi & A. Lotova, "Parallel-Connected Solar PV System to Address Partial and Rapidly Fluctuating Shadow Conditions," IEEE Trans. on Industrial Electronics, Vol. 56, No. 5, MAY 2009, pp. 1548-1556. H. Patel & V. Agarwal, "MATLAB-Based Modeling to Study
- the Effects of Partial Shading on PV Array Characteristics, IEEE Trans. on Energy Conversion, Vol. 23, No. 1, March 2008, pp. 302-310.
- A. Chouder & S. Silvestre, "Analysis Model of Mismatch Power Losses in PV Systems," Journal of Solar Engineering, May 2009,
- N. Femia, G. Lisi, G. Petrone, G. Spagnuolo & M. Vitteli, " Distributed Maximum Power Point Tracking of Photovoltaic Arrays: Novel Approach and System Analysis," IEEE Trans. on Industrial Electronics, Vol. 55, No. 7, July 2008, pp. 2610-2621.
- Y. Xue, L. Chang, S. Kjaer, J. Bordonau & T. Shimizu, Topologies of Single-Phase Inverters for Small Distributed Power Generators: An Overview," IEEE Trans. on Power Electronics, Vol. 19, No. 5, Sept. 2004

- J. Young-Hyok, K. Jun-Gu, P. Sang-Hoon, K. Jae-Hyung & W. Chung-Yuen, "C-language Based PV Array Simulation Technique Considering Effects of Partial Shading," International Conference on, Industrial Technology(ICIT), 2009, pp. 1-6.
- R. Bruendlinger, B. Bletterie, M. Milde & H. Oldenkamp, 'Maximum Power Point Tracking Performance Under Partially Shaded PV Array Conditions," Proceedings of the 21st European PVSEC, Dresden, 2006.
- R. Ramabadran & B. Mathur, "Effect of Shading on Series and Parallel Connected Solar PV Modules". Modern Applied Science, Vol. 3, N010, October 2009, pp. 32-41.
- M. Garcia, J. Maruri, L. Marroyo, E. Lorenzo & M. Perez,"Partial Shadowing, MPPT Performance and Inverter Configurations: Observations at Tracking PV Plants," PROGRESS IN PHOTOVOLTAICS: RESEARCH AND APPLICATIONS, April 2008, pp. 529-536.
- U. Schwabe & P. Jansson, "Performance Measurement of Amorphous and Monocrystalline Silicon PV Modules in Eastern U.S. Energy production versus ambient and module temperature," I2MTC 2009 - International Instrumentation and Measurement Technology Conference, Singapore, 5-7 May 2009
- S. Krauter, A. Preiss, N. Ferretti &P. Grunow "PV Yield Prediction For Thin Film Technologies and the effect of input parameters inaccuracies, 23rd European Photovoltaic Solar Energy Conference, Valencia, Spain, 1-5 September 2008.
- http://www.steveransome.com/pubs.html
- http://enphaseenergy.com/support/learningcenter.cfm
  R. Adler, "A New DC-DC switching Regulator Topology Enhances Efficiency and Power Density," Proceedings of PowerCon 1984, pp. F1-1-F1-4.
- Min, J. Lee, J. Kim, T. Kim, D. Yoo & E. Song, "A New Topology With High Efficiency Throughout All Load Range for Photovoltaic PCS," IEEE Transactions on Industrial electronics, Vol. 56, No. 11, Nov. 2009, pp. 4427-4435.
- H. Li, H. Chen & L. Chang, "Analysis and Design of a Single-Stage Parallel AC-to-DC Converter," IEEE Transactions on Power Electronics, Vol. 24, No. 12, December 2009, pp. 2989-
- M. de Rooij, J. Glaser & R. Steigerwald, "High Efficiency Photovoltaic Inverter," US patent application # US2009/0323379
- [21] R. Steigerwald, M. Agamy, M. Harfman-Todorovic, A. Elasser & J. Sabate, " Dc to Dc Power Converters and methods for controlling the same," US patent application # US2012/0051095
- A. Min, J. Lee, J. Kim, T. Kim, D. Yoo & E. Song, "A New Topology With High Efficiency Throughout All Load Range for Photovoltaic PCS," IEEE Transactions on Industrial electronics, Vol. 56, No. 11, Nov. 2009, pp. 4427-4435.
- M. Agamy, M. Harfman-Todorovic, A. Elasser, J. Sabate, R. Steigerwald, Y. Jiang & S. Essakiappan," DC-DC Converter Topology Assessment for Large Scale Distributed Photovoltaic Plant Architectures," Proceedings of ECCE 2011, pp. 764-769.

Disclaimer: This report was prepared as an account of work sponsored by an agency of the United States Government. Neither the United States Government nor any agency thereof, nor any of their employees, makes any warranty, express or implied, or assumes any legal liability or responsibility for the accuracy, completeness, or usefulness of any information, apparatus, product, or process disclosed, or represents that its use would not infringe privately owned rights. Reference herein to any specific commercial product, process, or service by trade name, trademark, manufacturer or otherwise does not necessarily constitute or imply its endorsement, recommendation, or favoring by the United States Government or any agency thereof. The views and opinions of authors expressed herein do not necessarily state or reflect those of the United States government or any agency thereof.